A New Modeling and Simulation CAD Package for Power Converter Design

SANTIAGO LORENZO, MEMBER, IEEE, JOSÉ MIGUEL RUIZ, FERNANDO ALDANA, SENIOR MEMBER, IEEE, AND MAHMOUD SHAKER

Abstract—**The application of CAD technology to simulation, modeling, and design of any system eliminates the difficulties and improves the results obtained by the use of traditional mathematical approaches. The actual work presents a new CAD package to be used for modeling, simulation, and design of digitally controlled static power converters [1], [7], [8], [28], [31], [32]. A real structure simulation for a matrix and no matrix (switched mode) converter is presented. The system modeling and identification is also presented as a new way to design digital controllers that are MP based. The present work follows the new digital simulation and redesign concept [30] and is a complementary continuation of [8], [28], [31], and [32].**

I. Introduction

COMPUTER simulation is currently a regular tool to be used in every engineering field; nevertheless, most power electronic equipment has been designed via prototype, and the reasons for this are clear: The existence of general purpose tools (oscilloscopes, registers, etc.), as well as the possibility of making reduced scale prototypes, facilitate the task. On the other side to the moment of personal computer (PC) availability, most computers have been used only with a numerical, and not a graphical, capability, which is, in simulation, critically necessary.

Some important questions have to be answered in this paper: Why is simulation used; why is real structure simulation better; why use digital modeling and identification. Some answers follow:

1) If power electronics is among the fields in which the design via scale-reduced prototype is easy, the prototype has to be made and tested from the initial design steps. The simulation approach avoids all kinds of equipment construction until the designer knows the construction and most problems have been solved. The prototype implementation will only show practical aspects.
2) The above-described simulation is a practical tool (only in the way in which it will show what happens) and is as close as possible to the real physical phenomenon. Our real structure simulation (RSS) presented here shows the signals as real ones; therefore, the difference between the simulated and the real magnitudes is almost null, and because of that, it is also possible to proceed to system identification and modeling.
3) The traditional way to design in power electronics can be called the approximate one because the model's mathematical estimation gives a poor description of the system. The actual availability and low price of MP-based digital controllers imposes the need of digital system modeling; the systems to be controlled can no longer be studied like analog but must be studied as digital, and because of that, digital identification is necessary.

The RSS simulation and digital identification described here are the two most powerful tools of power electronics computer aided design and simulation, (PECADS), which is an integrated PC-based CAD package that has been described [8], [28], [31]. Here, we will review what the simulation and modeling applies to.

II. Simulation

The simulation package follows the RSS rule that each block has to be simulated in such a manner that the output signals will represent the same evolution as the real ones. In that way, the difference between the PC and the oscilloscope signals is null (a high-resolution-screen PC has been used), and only the speed is lower. The package has three main functions:

1) Converter + plant steady-state simulation
2) converter + plant dynamic simulation
3) controller + converter + plant closed-loop simulation.

The first two will be individually studied.

A. Converter + Plant Steady-State Simulation

At this point, we should make a new converter classification.

a) Matrix-type converters (MTC's): In this type (Fig. 1(a)), the general converter configuration can be represented as a switching matrix [4], [5]. The switching matrix represents the simplest conceivable switching converter topology that performs the most general conversion function, and no components except switches are connected between the input and the output sources.

b) No matrix-type converters (NMTC's) or switched mode power converters: This second type also has a set of

Manuscript received September 9, 1987; revised May 1, 1990.

S. Lorenzo, J. Ruiz, and M. Shaker are with the Departamento de Electronica, Escuela Técnica Superior de Ingenieros Industriales, Valladolid, Spain.

F. Aldana is with the Departamento de Electronica, Escuela Técnica Superior de Ingenieros Industriales de Madrid, Madrid, Spain.

IEEE Log Number 9038044.

0278-0046/90/1000-0387$01.00

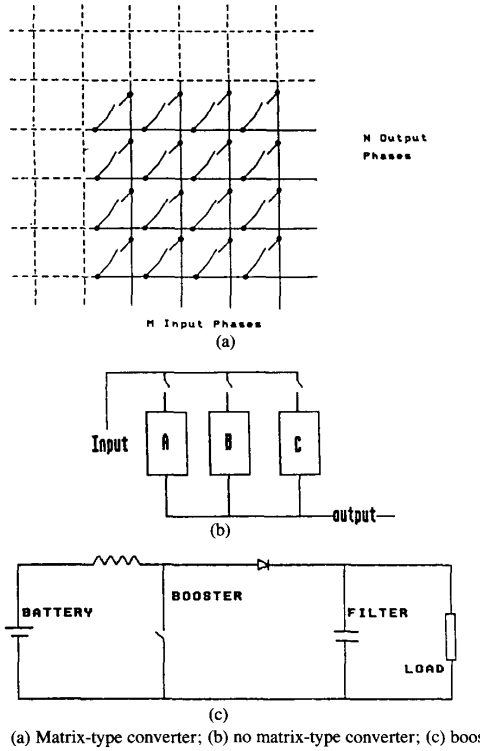

Fig. 1. (a) Matrix-type converter; (b) no matrix-type converter; (c) booster.

switches that connect input and output sources, but it also has a second set of reactor capacitors and resistors, which really perform the converter function. Fig. 1(b) shows a general topology of the NMTC, where the switch operations give different circuit configurations. Fig. 1(c) shows a booster as example of the NMTC.

1) Matrix-Type Converter Simulation: The converter simulation for the MTC is made according to [1], [2], and [3], using the existence function theory [4], [5]. In that theory, every converter is considered to be controlled by switching matrix modulation. Each individual switch has a switching pulse pattern ("0" open "1" closed), which can be modulated on the following:

1) Phase displacement (h/M): ac/dc and cycloconverters
2) pulse pattern frequency (w): harmonic composition
3) pulse width (A): PWM dc/ac and dc/dc converters
4) combination of the above modes.

According to [1] and [4], the output voltages V_j and input currents I_i can be expressed by (2), (3), where H_{ij} and H are the individual switch existence function and the converter existence function matrix, respectively. To generate the switching patterns, output magnitudes, and to analyze the harmonics content (using for example FFT), the PC has been adopted as an actual general purpose tool.

$$V_j = \sum_1^M H_{ij} \cdot V_i; \quad I_i = \sum_1^M H_{ij} \cdot I_j \tag{1}$$

$$[V_{\text{out}}] = [H] \cdot [V_{\text{in}}]; \; [I_{\text{in}}] = [H]^T \cdot [I_{\text{out}}]. \tag{2}$$

The existence function for an isolated switch is a pulse train, as shown in Fig. 2(a) and (b), which has been mathematically described as a Fourier expansion (3) and is easily simulated as shown in Fig. 2. The PC flow chart diagram that generates the modulated existence function is presented in Fig. 2(d), where a truncation at 0.5 with only a 10-term expansion, gives timing errors less than 1/1000 over the PWM's most narrow pulse:

$$H_{ij} = 1/A + (2/\pi) \cdot \sum_1^\infty \left[\sin(n \cdot \pi/A)/n\right] \cdot \cos(nwt + M). \tag{3}$$

Fig. 2(a) shows the switching patterns for a modulation index (x) = 0.6 and a frequency modulation ratio (FMR) = 9, for a PWM converter. In Fig. 2(b), a periodic pulse train has also been represented, and in Fig. 2(c) the PWM first five harmonics has been plotted to clearly demonstrate the two reasons why the 0.5 truncation gives a good approximation; harmonics composition on (3) decreases on a $1/n$ rate; the n order is a multiple of the very high w carrier frequency because the harmonic zero crossover speed is extremely high.

The PC simulation described gives a very-high speed (several seconds in every screen), but in order to have an instantaneous simulation, the existence function can be pregenerated and stored at the PC memory via a file; in that case, from the user's point of view, every phenomena happens in a real time scale.

More details over the existence functions, voltages, and current generation can be found in [1], [2], and [3]; here, we only show two typical simulations: ac/dc converter in Fig. 3(a) and dc/ac converter in Fig. 3(b), where the upper and lower sections are different CAD utilities, which can be combined with several others (average, RMS, and maximum values and DFT analysis of input and output voltages and currents, time evolution of voltages, currents and power for the power poles, power factor, and distortion) having, in total, a multitool functionality.

The plant simulation is done by following the discretization techniques (Euler and others) in a block by block manner; therefore, the computer will solve the differential equations that once were transformed in difference equations. The $G(s) \rightarrow G(z)$ transformation is quite simple because the elementary block configuration (integral, time constant, etc.) and all internal and external magnitude evolutions can be graphically represented, as in the real system.

2) No Matrix (Switched Mode)-Type Converter Simulation: The Converter simulation of the NMTC is made with a rather different approach. In the most general case, a NMTC is defined [9], [10], [11], [31] by a set of differential and constraint equations (4), where x is the state vector, p the controlling parameter, and T the time transition vector, and these define the state functionality and the transition between states. A general diagram has been represented in Fig. 4(a), where several timing-controlled switches (t_1 to t_n) switch the differential equations set (A, B, C, $\cdots$) in a 0–T period.

By partitioning the repetition period T into single subinter-

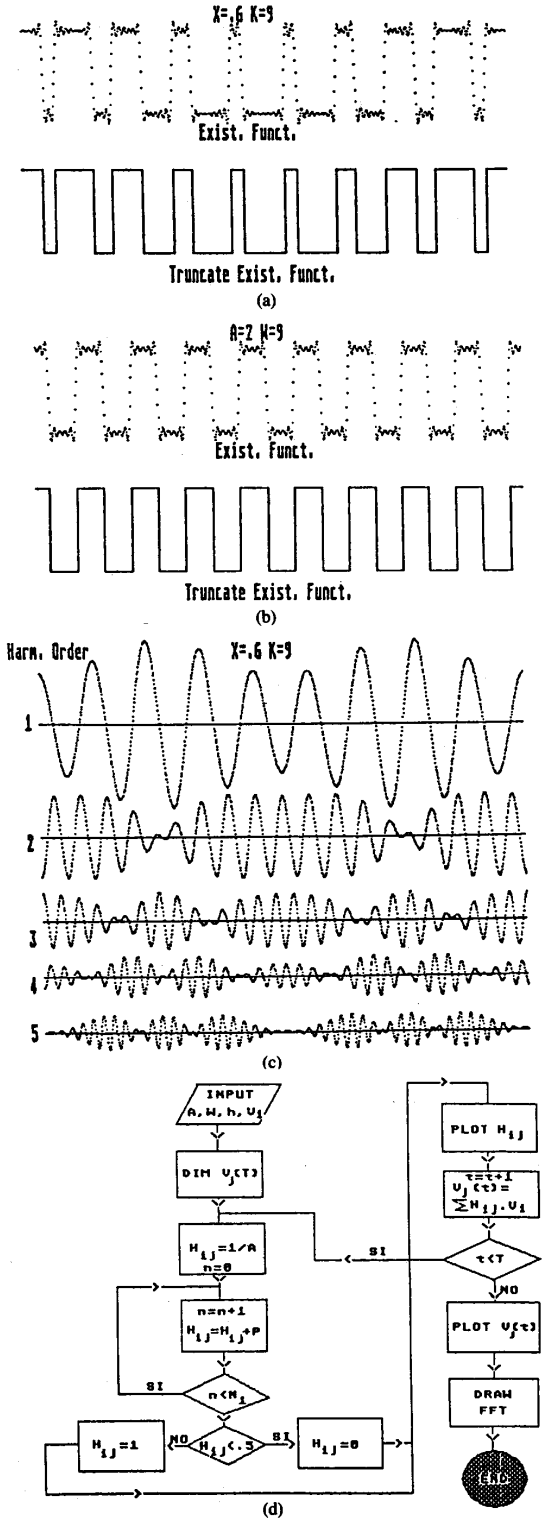

Fig. 2. (a) PWM pulse train; (b) periodic pulse train; (c) first five harmonic representation of the PWM pulse train; (d) PC simulation flow chart.

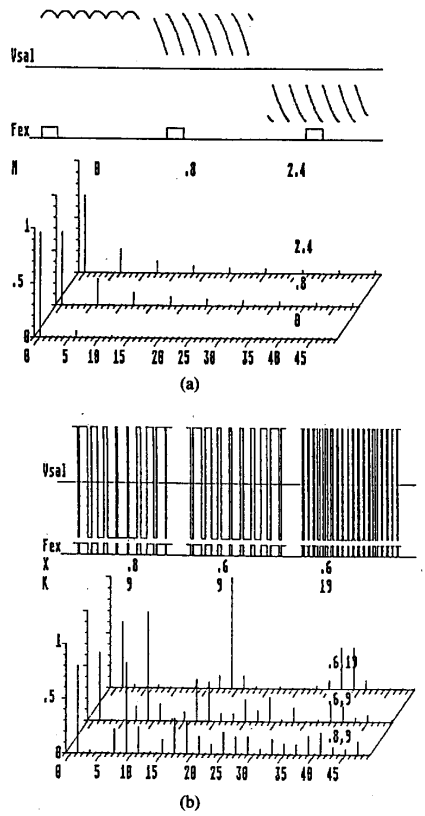

Fig. 3. (a) ac/dc converter simulation and FFT analysis; (b) dc/ac PWM converter simulation with FFT analysis.

vals t_i and designing with notation t_i each single switching point, for every subinterval (t_i, t_{i+1}), the system behavior is governed by a different set of differential equations:

$$dx_i/dt = f_i(x_i, u, t); \quad x_i(t_i) = x_{io}; \qquad c_{i+1}(x_i, u, t_{i+1}) = 0. \quad (4)$$

The latter determines the switching point t_{i+1} and can be considered to be the constraint equation.

One can see step by step in Fig. 4 how the simulation system solves (in a closed-loop mode) the differential equation blocks A, B, C, etc., which change from one to the other at the switching times and transfer the ending variable values in one state as the starting ones to the next in such a way that the variable's evolution is an exact physical phenomena representation. The converter simulation is done following the discretization techniques (Euler and others), and the computer runs over states A, B, C according to the controlled or natural switching cycles.

Now, as an example, we consider the Buck-boost converter, which is represented in Fig. 4(b). The possible circuit states A, B, C can be expressed as follows:

1) In the A state, the switch is closed so that the circuit differential equations become

$$E = dI_1/dt; \qquad I_c = C \cdot dV_0/dt. \quad (5)$$

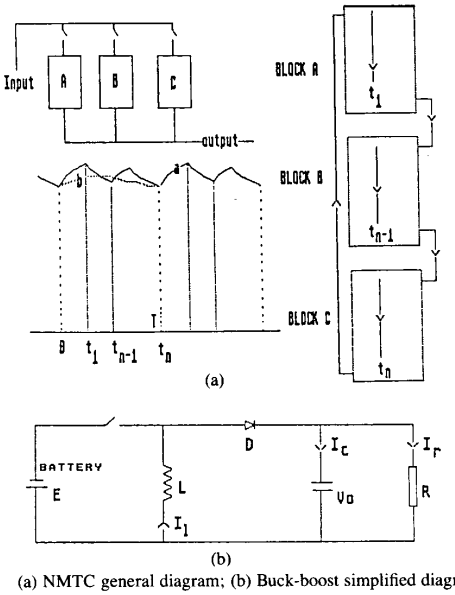

Fig. 4. (a) NMTC general diagram; (b) Buck-boost simplified diagram.

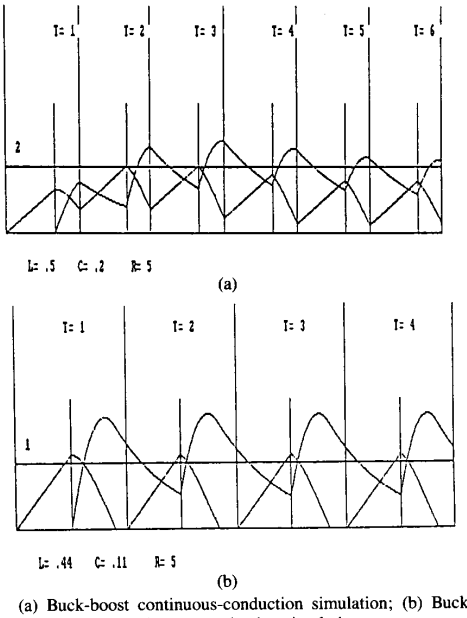

Fig. 5. (a) Buck-boost continuous-conduction simulation; (b) Buck-boost discontinuous conduction simulation.

2) In the B state, the switch is open, and the current flows from the reactor to the capacitor and load; the differential equations are

$$V_0 = L \cdot dI_1/dt; \quad I_c = C \cdot dV_0/dt; \quad I_1 = I_c + V_0/R. \tag{6}$$

3) In the C state, the current I_1 equals zero, D blocks the reverse flow, and the differential equations are

$$I_1 = 0; \qquad V_0/R = C \cdot dV_0/dt. \tag{7}$$

4) The converter gets only the states A and B in continuous conduction, which has been simulated out of scale, as is shown in Fig. 4(a), to show the physical situation.

5) The converter works in the three states A, B, C in discontinuous conduction, which has been simulated out of scale in Fig. 5(b).

Several works [9], [10] are based on the state-space exponential averaging matrix solution, but our *RS* simulation option, which is really useful for the simulation approach, followed by digital identification, forces us to do otherwise.

B. Converter + Plant Dynamic Simulation

There is a real need in our description to speak about RSS because of its block-by-block configuration and real output signal measurement, which really represents the magnitude's physical evolution, and is also a slow down real time simulation, because every phenomena happens in a real but slowed down mode. In Fig. 6(a), a ac/dc converter with dc motor load and phase displacement control RSS dynamic simulation is shown. In Fig. 6(b), a dc/ac inverter RSS dynamic simulation is shown when a reference step at the arrow position is applied. In Fig. 6(c), a boost converter simulation is shown with a reference step and minimal phase result.

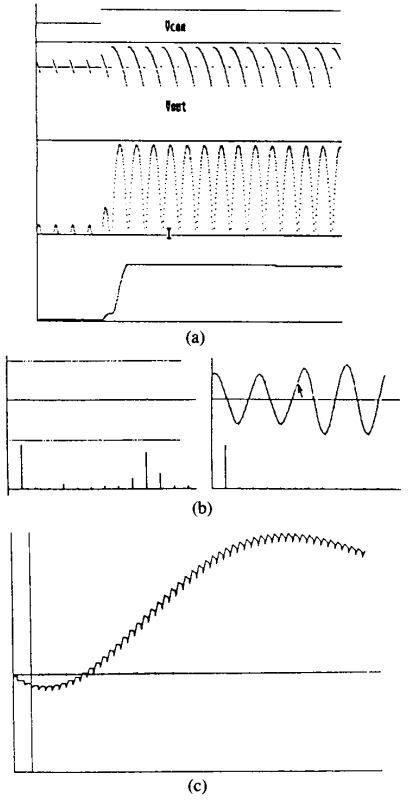

Fig. 6. (a) dc/dc converter plus dc motor RSS dynamic simulation; (b) dc/ac inverter dynamic simulation; (c) boost converter dynamic simulation.

III. Modeling

The traditional way to modeling in power electronics has been based on a mathematical definition that is followed by a complex mathematical formulation, which has been considered by us as an approximate way because it may give a system's dynamics poor description. In power electronics, the converter–plant transfer function is often not linear, and because of their mutual interaction, is no more the product of the converter and plant functions; NMTC multistage differential equations and discontinuous conduction in MTC are clear examples of traditional serious difficulties in mathematical modeling.

The RSS simulation described here allows us to proceed to the system identification with digital algorithms under different working conditions, which is a very accurate way, but it is not the only benefit; the main advantage is the possibility of knowing a discrete transfer function, as is required for digital controller design.

The digital identification used in this work employs the PC as the basic tool and directly gives the $F(z)$ converter-plant transfer function. We will follow with some explanations about the identification and modeling package.

Suppose we have a system $F(z)$, as represented in Fig. 7(a), which is composed for a power converter plus plant. According to the RSS described above, we can analyze their input $X(z)$ and their output $Y(z)$. If $F(z)$ has to be controlled by a digital system, their transfer function has the following expression (8):

$$ZB_0F(s) = (z^{-1})/z \cdot Z(F(s)/s). \tag{8}$$

For an "n" order system with a $h = T_r/T$ transport delay, and approaching the z transform by $F(z) = ZB_0F(s)$, (9), (10) and (11) may be applied:

$$ZB_0F(s) = z^{-h}\left(\sum_i^n Ai \cdot z^{-i}\right)\Big/\left(1 - \sum_i^n Bi \cdot z^{-i}\right) = F(z) \tag{9}$$

$$Y(z)/X(z) = F(z) \tag{10}$$

$$yk = B1 \cdot y(k-1) + \cdots Bn \cdot y(k-n) + A1 \cdot x(k-1) + \cdots An \cdot x(k-n). \tag{11}$$

According to Figs. 7(a) and 7(b), $B1$ to Bn and $A1$ to An can be calculated in a direct or recursive manner [19].

The time-domain choice instead of the frequency domain one has been used for the following reasons:

1) Power electronic systems can be easily simulated by the use of RSS algorithms [1]–[8], [31].
2) The RSS to an input step has, in most cases, a filtering type noise because of the known harmonics composition, therefore, the direct way, which is very fast and accurate (only a set of equations has to be solved by Gauss) can be used.
3) The time domain choice automatically gives the order of the system and the time of response.
4) The time domain choice could be implemented as in Fig. 7, in an interhelping mode between direct (Gauss) and recursive least squares (RLS) [14], [15] algorithms.

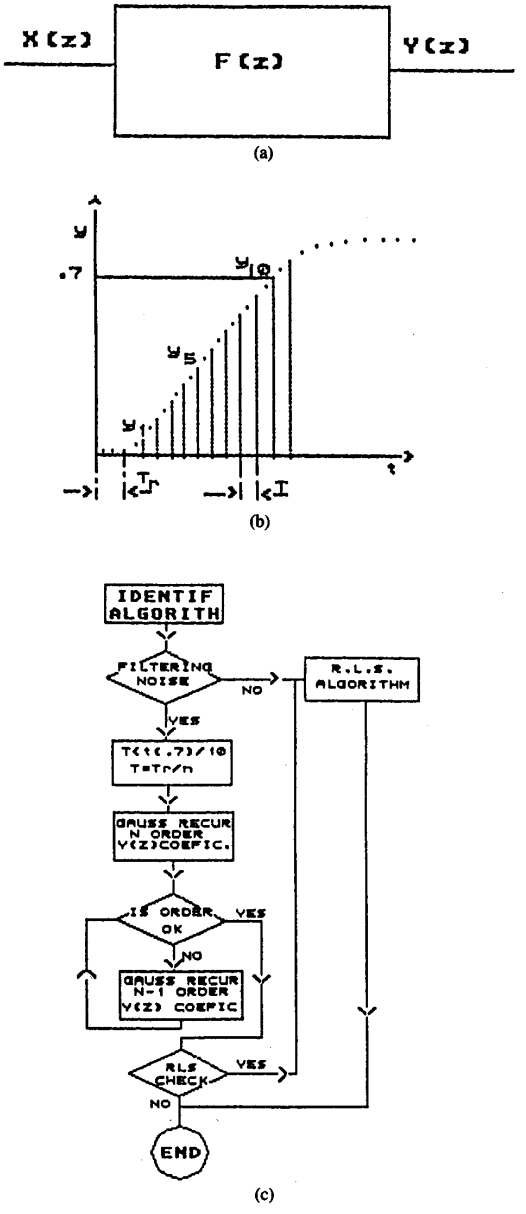

Fig. 7. (a) Converter-plant block diagram; (b) time response to a step; (c) identification flow chart.

As indicated in the identification flow chart, in the case of no or filtered noise, the computer reads a file with the stored output values and takes a sampling period T value with the following conditions: $T \approx tR/10$ (tR is the time of response to get 70% stationary); $T = Tr/h$ (T_r being the transport delay, h should be an integer), and use the number of points that is enough to identify the Ai Bi coefficients, solving the system of equations by Gauss. The CAD identification pro-

cess works as follows:

1) Calculate the Ai and Bi coefficients starting from the low (first) order and increasing.
2) For each order, compute the error between the simulated and the identified equations.
3) The system stops when the computed error is lower than a small fixed level and is the lower among the computed (all the small order and one high order) so that the error tendency changes after a minimum value.
4) The CAD gives, in the described way, the most accurate system order as well as its Z transform equation.

In the unfiltered noise case, the RLS algorithm has been used, starting nevertheless with the same T choice (the identification process is similar to the one above described) and having the possibility of step or white noise as the input signal used for identification. RLS identification means to minimize the root of the square of the error between the real output and the identified one. This algorithm [14], [15] is represented by equations (12) to (18):

$$\theta(t) = \theta(t-1) + L(t) \cdot \left[y(t) - \theta^T(t-1) \cdot \phi(t) \right] \tag{12}$$

$$L(t) = \left[P(t-1) \cdot \phi(t) \right] / \left[1 + \phi^T \cdot P(t-1) \cdot \phi(t) \right] \tag{13}$$

$$P(t) = P(t-1) - \left[P(t-1) \cdot \phi(t) \cdot \phi^T(t) \cdot P(t-1) \right] / \left[1 + \phi^T(t) \cdot P(t-1) \cdot \phi(t) \right] \tag{14}$$

$$y(t) = B1 \cdot y(t-1) + \cdots + Bn \cdot y(t-n) + A1 \cdot x(t-1) + \cdots A_m \cdot x(t-m) \tag{15}$$

$$y(t) = \phi^T(t) \cdot \theta^T(t);\ \phi^T(t) = (-y(t-1) \cdot \cdots - y(t-n), x(t-1) \cdots x(t-m) \tag{16}$$

$$\theta^T(t) = (-B1 \cdots - Bn, A1 \cdots Am) \tag{17}$$

The initial conditions are $P(0) = C \cdot I$, where I is the unit matrix, and C is some large constant $\theta(0) = 0$; $P(t)$ and $L(t)$ are the operating matrices, and the final equation (18) is a Z transform of (11):

$$G(z) = \left[A1 \cdot z^{-1} + A2 \cdot z^{-2} + \cdots An \cdot z^{-n} \right] / \left[1 - B1 \cdot z^{-1} - B2 \cdot z^{-2} - \cdots - B_n \cdot z^{-n} \right]. \tag{18}$$

At this point, we should analyze the different types of systems that can be found in power electronics to know if all of them can be expressed by a single Z-transform equation. We will refer to the single input single output (SISO) systems, but the conclusions can be extended to the multiinput multioutput (MIMO) systems.

Any kind of linear system can be expressed by general $G(s)$ and $G(z)$ equations; the first question is what happens if the system is nonlinear? Generally, any nonlinear system with a unique differential equation set and variable parameters can be approximated by a linear one when a small disturbance is applied around each working point; it can therefore be identified in a step-by-step sequence.

The second question to be solved here refers more to the case in which the system is not described by a singular differential equation set but for several sets of them (one by state), which is the case in NMTC (switched mode converters) and some special cases (discontinuous conduction and others) in MTC (matrix converters).

The sampled data description for a switched-mode converter operating over a cycle will be performed by a succession of N equations, as previously suggested, in the form

$$x(t_{k+1}) = f(x(t_k), p_k, T_k) \tag{19}$$

$$c(x(t_k), p_k, T_k) = 0. \tag{20}$$

One set for each of the N switch configurations is in the cycle. The evolution is continuous across each change in switch configuration, i.e., the final value in one configuration is the initial in the next.

Equation (20) summarizes the constraint equation for each mode. T_k represents the transition times vector governed directly or indirectly by a set of controlling parameters p_k. The transition times may be directly controlled by external control action, or the transition can occur when the system values reach particular levels or threshold conditions.

To provide a concrete example, suppose a NMTC is the one represented in Fig. 4(a). In each state $0/t_1 \cdots t_{n-1}/tn$, a different set of differential equations applies, and one can say no singular differential equation set can describe the full system functionality.

Let us suppose a linear description in a multistate system as presented in Fig. 4(a) with only three states. The successive difference equations (21)–(23) describe the signal evolution (curve "a" in the figure) over a period:

$$(0 - t_1) \quad y(k) = B_{11} \cdot y(k-1) + \cdots + B_{n1} \cdot y(k-n) + A_{11} \cdot x(k-1) + \cdots + A_{m1} \cdot x(k-m) \tag{21}$$

$$(t_1 - t_2) \quad y(k) = B_{12} \cdot y(k-1) + \cdots + B_{n2} \cdot y(k-n) + A_{12} \cdot x(k-1) + \cdots + A_{m2} \cdot x(k-m) \tag{22}$$

$$(t_2 - t_3) \quad y(k) = B_{13} \cdot y(k-1) + \cdots + B_{n3} \cdot y(k-n) + A_{13} \cdot x(k-1) + \cdots + A_{m3} \cdot x(k-m). \tag{23}$$

If the sampling time for the three equations is T_m, the final value at the end of the cycle will be the same with the full set working from 0 to t_3 but with the new individual sampling times expressed by (24):

$$T_{m1} = T_m(t_1 + t_2 + t_3)/t_1; \quad T_{m2} = T_m(t_1 + t_2 + t_3)/t_2; \quad T_{m3} = T_m(t_1 + t_2 + t_3)/t_3. \tag{24}$$

Now, according to the z algebra, a new common sampling time T_{mx} can be used for the full equations set (21)–(23), from 0 to t_3, but the coefficients A_i to B_i become modified to the new a_i to b_i in (25)–(27):

$$y(k) = b_{11} \cdot y(k-1) + \cdots + b_{n1} \cdot y(k-n) + a_{11} \cdot x(k-1) + \cdots + a_{m1} \cdot x(k-m) \tag{25}$$

$$y(k) = b_{12} \cdot y(k-1) + \cdots + b_{n2} \cdot y(k-n) + a_{12} \cdot x(k-1) + \cdots + a_{m2} \cdot x(k-m) \tag{26}$$

$$y(k) = b_{13} \cdot y(k-1) + \cdots + b_{n3} \cdot y(k-n) + a_{13} \cdot x(k-1) + \cdots + a_{m3} \cdot x(k-m). \quad (27)$$

Finally, because of the common sampling time T_{mx}, a single equation (28) could represent the system over the period:

$$y(k) = B_1 \cdot y(k-1) + \cdots + B_n \cdot y(k-n) + A_1 \cdot x(k-1) + \cdots + A_m \cdot x(k-m). \quad (28)$$

Thus, we can approach the behavior modeling the system as a single unity. If the model starts with the initial value of the switched circuit at the beginning of the period, its evolution would intersect that of the switched circuit at all multiples $k \cdot T$ (k integer) of T, where T denotes the operating period. It is also not hard to show that if the model were started at the same time t_x as the switched system, then its evolution would intersect that of the switched system at the instants $t_x + T$.

For these converters, the switching frequencies are usually considerably higher than the natural frequencies of the circuit configuration. As a result, by this way, it is possible to replace instantaneous values by average values. The approach can be extended for a small signal and results in linear approximation of the system dynamic evolutions. The model describes the evolution of the system in terms of samples taken every cycle. The main objective of the CAD is to provide a model that satisfactorily approaches the system that will be used to design the regulator. In this sense, all the controlling parameters are constrained to vary no more frequently than once per cycle.

In short, because of the linear approximation of the system evolution, with sampling time equal to the operation period, (19) is linear, and a relation similar to (28) can be expressed for Tk_i instead of $x(k_i)$. In addition, the considerations exposed in terms of samples taken every cycle can be extended to sampling times bigger than the operation period if the system dynamic is slow enough.

The RSS simulation followed by identification can provide this model. Obviously, the approach process can be more exact by other different methods [9], [10], [11] but can be quite time consuming and may lead to models that are unnecessarily complex regarding our objectives. The initial simplicity and the generalization of the proposed procedure makes it desirable, and we may decide to use it at the CAD like a tool.

To give a physical feeling of the above conclusion and to show the CAD potentiality, the Fig. 4(a) buck-boost inverter has been simulated. Fig. 8(a) shows the output voltage and current signals, and Fig. 8(b) shows the identification process (continuous line is the simulated system; the dotted lower line is the identified system as a first order; the dotted upper line is the same as a second order, which is the selected one). We should remark that the identified system has also been represented in Fig. 8(a) (continuous line), showing the total identity between the simulated and the identified system. As can be seen in Fig. 8(b) (lower), the CAD gives the Z-transform

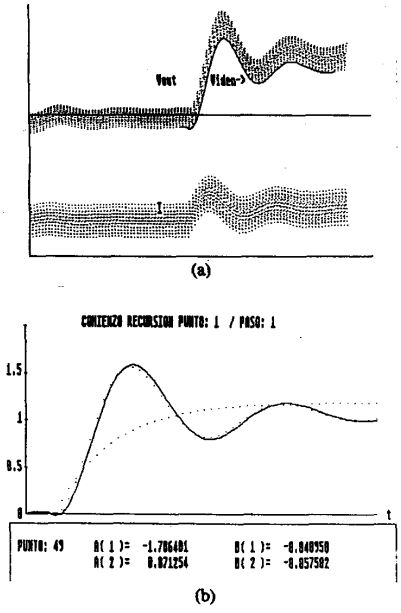

Fig. 8. (a) Output voltage and current for a Buck-boost converter (the continuous line is the identified system simulation); (b) system identification as a second-order minimal phase one. The continuous is the simulated system; the dotted lower line identifies the first-order system; the dotted upper line identifies the second-order system.

equation:

$$G(z) = \frac{B(1) \cdot z^{-1} + B(2) \cdot z^{-2}}{1 + A(1) \cdot z^{-1} + A(2) \cdot z^{-2}}. \quad (29)$$

The above systems are cyclical over the T period; therefore, the same approach done for the 0 and T points can be done for any $0 + t_x$ and $T + t_x$ point as well as for the cyclic average value, which is a very important propriety for the systems in which the output controlled signal (voltage or current) is needed in dc form, which is the case in any type of ac/dc or dc/dc converter. In Section IV-C and Fig. 11, these conclusions are shown.

Once the $F(z)$ transfer function for the converter–plant system is modeled, it is really easy to design the digital controller regulator. The bilinear $z \rightarrow w$ transformation as well as the $z = e^{jwt}$ one has been used, but because of the possibility of direct synthesis design for digital regulators, modern algorithms like Kalman, dead-beat, Truxal minimal prototype, minimal response [16]–[18], and the new minimal response sliding (MRS) and minimal response integral sliding (MRIS) has also been included at PECADS in a constant or adaptive configuration.

It will be interesting to use the frequency domain techniques because the $z \rightarrow w$ (e^{jwt} type is preferred) PC-aided transformations are used to plot the discrete Bode or Nyquist charts. For nonlinear or VSS systems, a Bode-area plot, more than a singular curve, will appear, giving the opportunity to use MP look up table-based adaptive controllers or the traditional single configuration ones with slow response.

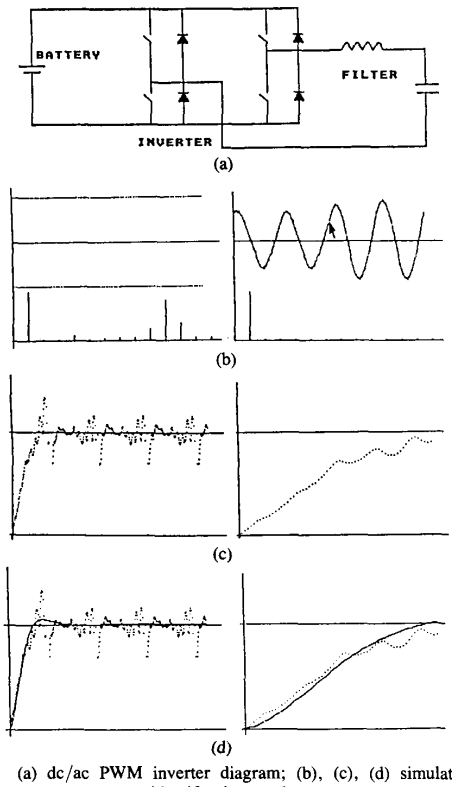

Fig. 9. (a) dc/ac PWM inverter diagram; (b), (c), (d) simulation and identification results.

IV. Modeling Examples

To give a real feeling about how the simulation and modelling-identification packages work, we follow three examples.

A. dc / ac PWM Inverter

A single-phase PWM dc/ac inverter is shown in Fig. 9. A step has been done at the "arrow" position, and the system has been identified as a second-order one. Because of the sinusoidal output voltage, a division by $\sin \alpha$ is necessary, and because of that, an unpredictable noise is present. The RLS algorithm has been used with good results.

B. dc / dc Buck-boost Inverter

A dc/dc Buck-boost inverter (Fig. 4(b)) has been identified as a second-order one with no minimal phase. In this case, because of the filtering noise output signal, the direct identification method has been used for a reference step. Because it is a switched-mode converter with multimode states and nonlinear configuration, it is a good example for analysis:

1) The identification process has been expanded to all continuous and discontinuous conduction cases.
2) The current has been selected as the parameter to control the transfer function modification.
3) In Fig. 10(a), the three most critical cases, which represent the limit between continuous and discontinuous conduction, have been selected: Continuous conduction (L = 17 Ω, I = 12.94 A); discontinuous conduction (L = 19 Ω, I = 11.57 A); limit between continuous and discontinuous conduction (L = 18 Ω, I = 22 A).
4) In Fig. 10(b), the obtained gain and phase Bode charts, from .1 Ω⟨⟩2200 A to 100 Ω⟨⟩2.2 A, are presented, and they surpass the range of practical cases.
5) Table I shows a complete set of "z" transform coefficients $K1$ to $K4$, according to formula (30), which will allow the design of an adaptive digital controller:

$$GR = \frac{K2 \cdot z^{-1} + K1 \cdot z^{-2}}{1 - K4 \cdot z^{-1} + K3 \cdot z^{-2}}. \qquad (30)$$

C. ac / dc Converter Plus dc Motor

It is a well known fact for all power electronics specialists that it is difficult to model the dc motor that is controlled via an ac/dc converter. Several works have been devoted to finding an accuracy transfer function for both continuous and discontinuous conduction; here, we will check the PECADS validity identification of such a system. In Fig. 11(a), a discontinuous conduction simulation has been plotted. A control step linearized arccosinus has been done, the "instantaneous average" (new concept introduced by us) current has been taken as an output, and the result of identification as a second-order system is shown in Fig. 11(c). The "z" equation coefficients are indicated at the same plot according to (29), and the accuracy of the identification can be verified (upper dotted line is identified to be second order, and the continuous line is the simulated system).

In Fig. 11(b), a continuous conduction simulation has been plotted. A control step linearized arccosinus has been done, the instantaneous average current has been taken as an output, and the result of identification as a second order system is shown in Fig. 11(d). The "z" equation coefficients are indicated in the same plot according to (29), and the accuracy of the identification can be verified (upper dotted is identified to be second order, and the continuous line is the simulated system).

As a final output, the Bode diagrams (phase upper and gain lower) have been plotted in Fig. 12 for the following conditions: (a) Discontinuous conduction in the no-transport delay case, (b) discontinuous conduction with a 60° transport delay, (c) continuous conduction with no transport delay, and (d) continuous conduction with a 60° delay. Looking at the results shown as well as others not shown here because of space limitations, one can conclude some interesting outputs, which follow:

1) In both cases, the actual transfer function will be placed between the A & B or C & D curves. No possibility appears to check the exact position, which depends on the Statistical Transport Delay.
2) The transfer function in the continuous conduction case, will change with the armature parameters La & Ra.
3) The transfer function in the discontinuous conduction

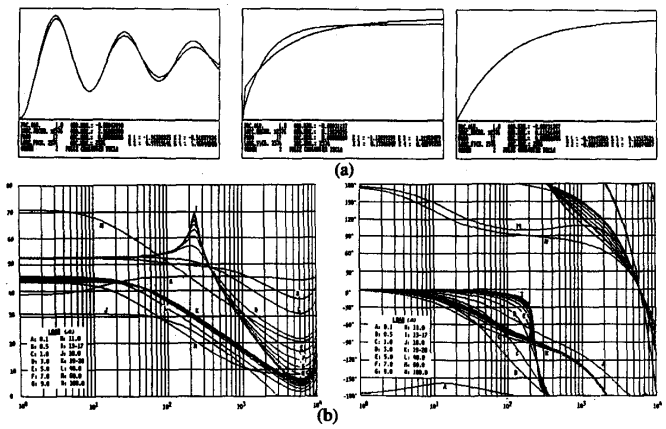

Fig. 10. (a) dc/dc Buck-boost converter simulated and identified systems; (b) Bode chart for the same system in continuous and discontinuous conduction.

TABLE I
COEFFICIENTS OF Z TRANSFER FUNCTION FOR A BUCK-BOOST CONVERTER

CURRENT (A)	K1	K2	K3	K4
2200	169.159042	-169.953308	.082022	-1.072799
440	113.064598	-108.217255	.600308	-1.588537
220	66.356567	-60.794945	.772363	-1.759443
73	25.543406	-19.494827	.917315	-1.903468
44	16.411831	-10.251558	.949068	-1.934981
32	12.348511	-6.138378	.962908	-1.948697
25	9.923892	-3.717742	.970704	-1.956420
20	8.266803	-2.113834	.975726	-1.961397
16.29	7.003555	-.920474	.979950	-1.965584
15.17	6.722180	-.663266	.981239	-1.966863
14.19	6.618780	-.520572	.982370	-1.967986
13.75	6.611526	-.492392	.982882	-1.968493
11	3.752545	.151613	-.001619	-.973190
7.85	3.027725	.269396	-.001698	-.980252
3.66	1.897905	-3.131637	.001293	-.992860

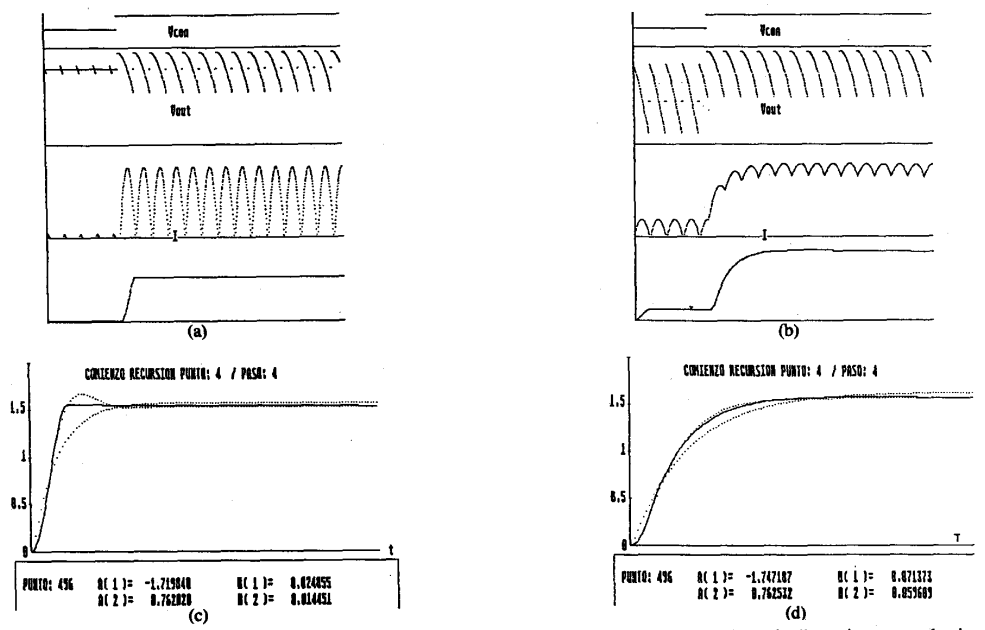

Fig. 11. ac/dc converter plus dc motor simulations and identifications: (a) Response to a control step in discontinuous conduction; (b) response to a control step in continuous conduction; (c) system identification in discontinuous conduction as a second-order one. The continuous line is the simulated system, the dotted lower line is first order, and the dotted upper line is second order; (d) system identification in continuous conduction with the same comments as above.

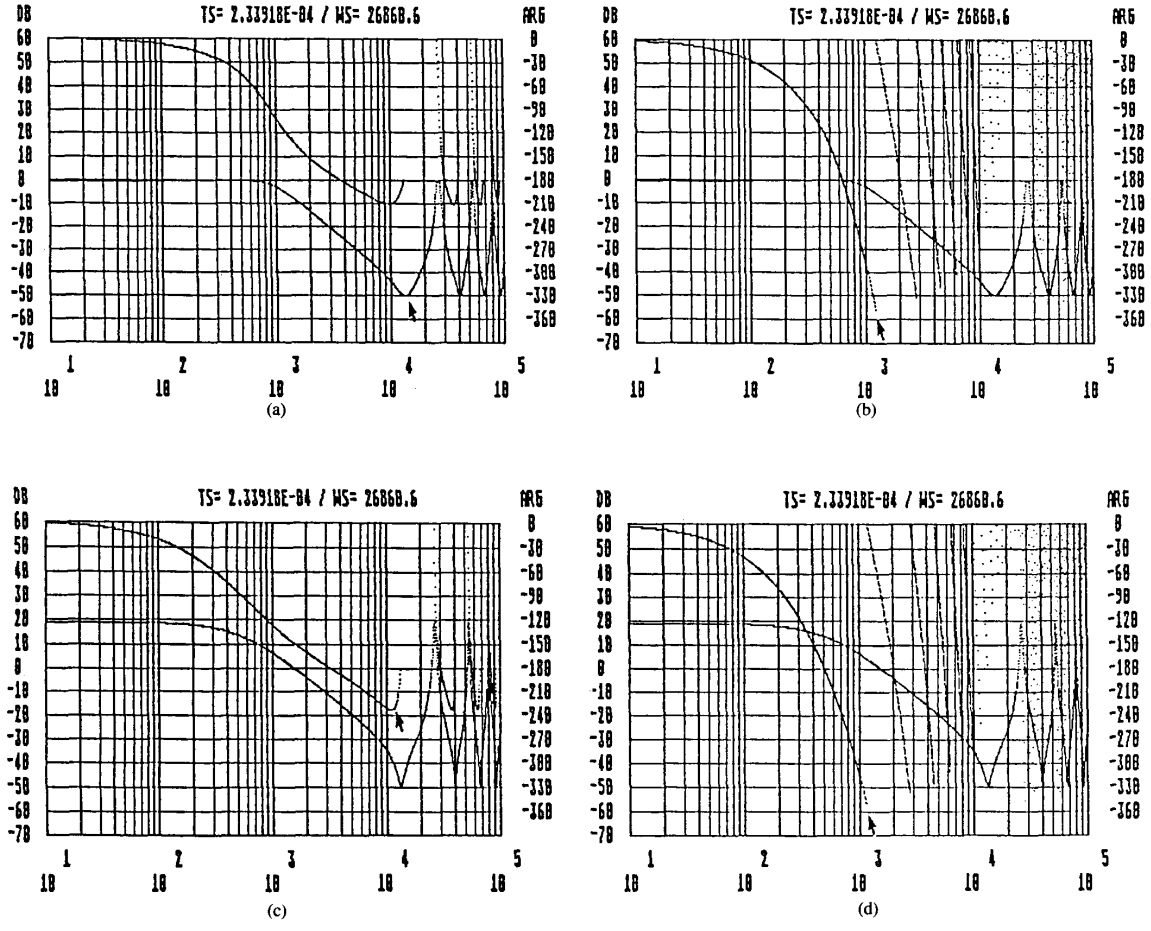

Fig. 12. Several Bode charts for a dc motor controlled by an ac/dc converter: (a), (b) discontinuous conduction without and with transport delay; (c), (d) continuous conduction without and with transport delay.

case, will change the gain according to the amount of discontinuity, but its corner frequency will stay at the same position.

4) A continuous–discontinuous conduction detection with a look-up table can be used to optimize the digital controller design in order to improve the overall system response.

V. Conclusions

The PECADS software CAD package described here is a powerful PC-based tool, which is used in the study and design of power electronics, in which a new real structure simulation concept has been developed; the system has the capability for steady-state simulation, which allows topology election, FFT analysis, etc., and for slow down real time simulation, which allows system identification, digital regulator synthesis, and closed-loop system simulation.

The full PECADS package also includes power semiconductors, protection sizing (using the magnitudes simulation capability), and a dedicated expert system that generates the most adequate switching pattern sequence for every application. The total system is fully open to new expansion or improvement.

References

[1] S. Lorenzo and J. M. Ruiz, "Power electronics system simulation using personal computers," in *Proc. IECOM'86* (Milwaukee), 1986.

[2] S. Lorenzo and J. M. Ruiz, "Simulacion de Convertidores de Potencia con PC I," *Mundo Electron.*, vol. 169, Jan. 1987.

[3] S. Lorenzo and J. M. Ruiz, "Simulacion de Convertidores de Potenencia con PC II," *Mundo Electron.*, vol. 171, Mar. 1987.

[4] P. Wood, *Switching Power Converters*. New York: Van Nostrand Reinhold, 1981.

[5] L. Giugyi, "Generalized theory of static frequency changers," Ph.D. thesis, Salford Univ. England, 1970.

[6] M. Shaker, S. Lorenzo, and J. M. Ruiz, "The use of PC in education field," in *Proc. MIMI'87* (El Cairo, Egypt), 1987.

[7] S. Lorenzo, M. Shaker, and J. M. Ruiz, "Real structure simulation and modeling in power electronic systems," in *Proc. IMACS'87* (Barcelona, Spain), 1987.

[8] S. Lorenzo, M. Shaker, and J. M. Ruiz, "PECADS an integrated CAD package to design power electronic systems and their MP based control," in *Proc. SICE'87* (Hiroshima, Japan), 1987.

[9] G. C. Verghese *et al.*, "A general approach to sampled-data modeling for power electric circuits," *IEEE Trans. Power Electron.*, vol.

PE-1, no. 2, Apr. 1986.
[10] R. D. Middlebrook and S. Cuk, "A general unified approach to modeling switching converter power stages," in *Proc. IEEE Power Electron. Spec. Conf.*, 1976.
[11] V. Vorperian and S. Cuk, "Small signal analysis of resonant converters," in *Proc. IEEE Power Electron. Spec. Conf.*, 1983.
[12] J. P. Louis, "Nonlinear and linearized models for control systems including static converters," in *Proc. IFAC Symp. Contr. Power Electron. Elec. Drives*, Sept. 1983.
[13] R. von Lutz and M. Grotzbach, "Straightforward discrete modeling for power converter systems," *IEEE Power Electron. Spec. Conf.*, 1985.
[14] D. Graupe, *Identification & Adaptative Filtering*. Malabar, FL: R. E. Krieger, 1984.
[15] L. Ljung, *Theory & Practice of Recursive Identification*. Cambridge, MA: MIT Press, 1983.
[16] S. Lorenzo, "Aplicacion de Microprocesadores a la realizacion de bucles discretos de control en Sistema Electronicos de Potencia," Ph.D. thesis, Escuela Super. de Ing. Industr., Madrid, Spain, 1983.
[17] S. Lorenzo, "Microprocesadores en reguladores industriales de potencia," *Mundo Electron.*, vol. 150, 152, Apr./May/June 1985.
[18] S. Lorenzo, "Realizacion de bucles discretos de control mediante microprocesadores en sistemas electronicos de potencia," in *Proc. VI Congreso de Automatic e Inform.* (Madrid), Oct. 1985.
[19] J. R. Leigh, *Applied Digital Control*. London: Prentice-Hall Int., 1985.
[20] O. Rubin, *The Design of Automatic Control System*. Norwood, MA: Artech House, 1986.
[21] U. Itkis, *Control Systems of Variable Structure*. New York: Wiley, 1976.
[22] F. Harashima, H. Hashimoto, and S. Hondo, "MOSFET converter position servo system with sliding mode control," in *Proc. IEEE Power Electron. Spec. Conf.*, 1983.
[23] F. C. Y. Lee *et al.*, "Generalized computer aided discrete time modeling and analysis of dc-dc converters," *IEEE Trans. Ind. Electron. Contr. Instrum.*, vol. IECM-26, May 1979.
[24] G. F. Franklin and J. D. Powell, *Digital Control of Dynamic Systems*. Reading, MA: Addison Wesley, 1980.
[25] K. J. Astrom and B. Wittenmark, *Computer Controlled Systems Design and Analysis*. Englewood Cliffs, NJ: Prentice-Hall, 1984.
[26] M. Shaker, S. Lorenzo, and J. M. Ruiz, "A new digital PWM strategy (Boxes Theory)," in *Proc. CAMC'87* (Minneapolis), June 1987.
[27] M. Shaker, S. Lorenzo, and J. M. Ruiz, "Digital PWM control for induction motor drives using boxes theory," in *Proc. SICE'87* (Hiroshima), July 1987.
[28] S. Lorenzo, M. Shaker, and J. M. Ruiz, "PECADS a new CAE simulation and design approach for static power converters," in *Proc. IAS Ann. Mtg.* (Atlanta), 1987.
[29] M. Shaker, S. Lorenzo, and J. M. Ruiz, "Microprocessor control for induction motors using boxes theory," in *Proc. IAS Ann. Mtg.* (Atlanta), 1987.
[30] B. C. Kuo, Digital Control Systems. New York: Holt-Saunders Int., 1980.
[31] S. Lorenzo, M. Shaker, and J. M. Ruiz, "PECADS an integrated CAE simulation and modeling package for static power converters MP controlled," in *Proc. IECON'87* (Cambridge, MA), 1987.
[32] M. Shaker, S. Lorenzo, and J. M. Ruiz, "Digital P.W.M. control for induction motor drives using boxes theory," in *Proc. IECON'87* (Cambridge, MA), 1987.